

Article

# A Semi-Simulated RSS Fingerprint Construction for Indoor Wi-Fi Positioning

Yuan Yang <sup>1,\*</sup>, Peng Dai <sup>1</sup>, Haoqian Huang <sup>2</sup> , Manyi Wang <sup>3</sup> and Yujin Kuang <sup>1</sup>

<sup>1</sup> Key Laboratory of Micro-Inertial Instrument and Advanced Navigation Technology, Ministry of Education, School of Instrument Science and Engineering, Southeast University, Nanjing 210096, China; 220173189@seu.edu.cn (P.D.); 220203602@seu.edu.cn (Y.K.)

<sup>2</sup> College of Energy and Electrical Engineering, Hohai University, Nanjing 210096, China; hqhuang@hhu.edu.cn

<sup>3</sup> School of Mechanical Engineering, Nanjing University of Science and Technology, Nanjing 210096, China; manyi.wang@njust.edu.cn

\* Correspondence: yangyuan@seu.edu.cn

Received: 21 August 2020; Accepted: 22 September 2020; Published: 24 September 2020



**Abstract:** Fingerprinting-based Wi-Fi positioning has increased in popularity due to its existing infrastructure and wide coverage. However, in the offline phase of fingerprinting positioning, the construction and maintenance of a Received Signal Strength (RSS) fingerprint database yield high labor. Moreover, the sparsity and stability of RSS fingerprinting datasets can be the most dominant error sources. This work proposes a minimally Semi-simulated RSS Fingerprinting (SS-RSS) method to generate and maintain dense fingerprints from real spatially coarse RSS acquisitions. This work simulates dense fingerprints exploring the cosine similarity of the directions to Wi-Fi access points (APs), rather than only using either a log-distance path-loss model, a quadratic polynomial fitting, or a spatial interpolation method. Real-world experiment results indicate that the semi-simulated method performs better than the coarse fingerprints and close to the real dense fingerprints. Particularly, the model of RSS measurements, the ratio of the simulated fingerprints to all fingerprints, and a two dimensions (2D) spatial distribution have been analyzed. The average positioning accuracy achieves up to 1.01 m with 66.6% of the semi-simulation ratio. The SS-RSS method offers a solution for coarse fingerprint-based positioning to perform a fine resolution without a time-consuming site-survey.

**Keywords:** indoor positioning; Wi-Fi fingerprinting; semi-simulated RSS; cosine similarity

## 1. Introduction

With the rapid development of indoor location-based service (LBS), several indoor positioning technologies have been proposed by researchers, i.e., wireless signal-based localization methods, ultrasonic positioning methods, and computer vision-based methods [1], etc. Among these alternative indoor positioning solutions, the wireless access technique of Wi-Fi has received much attention for its easy acquisition and wide coverage [2,3].

Wi-Fi fingerprinting positioning can be applied to any environment where APs are deployed sufficiently. What is more, Wi-Fi positioning accuracy is severely affected by real-world environments, i.e., varying multipath problems in dynamic environments [4]. Generally, there are mainly two ways to explore Received Signal Strength (RSS) to estimate users' positions. The first type is ranging-based WiFi positioning, using multi-lateration according to the estimated distance of target-APs (Access Points) pairs based on theoretical/experimental path-loss models. However, WiFi ranging in indoor environments confronts with heterogeneous distribution of high-dimensional RSS [5]. The second type is fingerprint matching by constructing RSS training dataset in an offline phase [6,7].

The training fingerprint dataset is established by scanning Wi-Fi signals from surrounding APs at site-surveying positions with corresponding labels (e.g., a grid point assigned with a unique label in this work) [8]. Besides, it has to survey all grid points, which is time-consuming and labor-intensive. The aforementioned methods of RSS fingerprint constructions take more effort than multi-lateration or connectivity-based localization methods, etc.

To overcome the limitations of Wi-Fi fingerprinting methods, researches proposed to reduce the complexity of fingerprint constructions. Talvite J. et al. [9] studied the performance of several interpolation and extrapolation methods for recovering the missing fingerprint data. Subarea strategies combined with data fitting methods were proposed in [10,11]. Jun J. et al. [12] designed a robust metric for fingerprinting in indoor localization named AP-Sequence, which reduced implementation overheads and ensured high accuracy by exploring the relative RSS difference among different APs [13]. Recent literature [14–17] proposed a scalable radio map, which divided the whole indoor area into multi-loop segments and acquired fingerprinting data rapidly. In [18], a modified Shepard's method estimated unknown Wi-Fi RSS values in the area with observation sparsity. Moreover, a method that trained the Wi-Fi fingerprint dataset using sensor-based navigation solutions was presented in [19]. Chen L. et al. [20] proposed a new algorithm based on an improved double-peak Gaussian distribution to generate the Wi-Fi fingerprints. The RSS approached in [21,22] applied to an interpolated dataset with the Kriging algorithm of the signal propagation characteristic (an inverse distance model).

In this work, we propose to simulate dense Wi-Fi RSS fingerprints from real measurements, consisting of two steps. Firstly, some nearby site-surveying grids of real coarse fingerprints are selected according to the cosine similarity. Then a signal path-loss model or quadratic polynomial fitting method [23] is applied to simulate the RSS value of the fingerprint at each non-site-surveying grid [24].

Comparing with the aforementioned spatial interpolations and signal propagation modeling, the proposed Wi-Fi fingerprint construction aims to simulate dense fingerprints from the real measurements of indoor scenarios. Therefore, the contributions of this paper are as follows.

- (1) The proposed semi-simulated construction is based on the real coarse Wi-Fi fingerprint dataset, which considers both real-world and simulated data. Therefore, the semi-simulated data is more accurate than other pure simulations.
- (2) Given the positions of APs, the cosine similarity is explored to select fingerprints for RSS estimation. It calculates the direction similarity between the coarse site-surveying grids and the simulated fingerprinting grids. Therefore, it makes these simulated fingerprints approximate the transmission loss in real-world environments as much as possible.
- (3) We employ a path-loss model, quadratic polynomial fitting method, or interpolation method for Semi-simulated RSS Fingerprinting (SS-RSS). The experiments, implemented in our small-scale indoor scenario, demonstrate that the quadratic polynomial fitting method performs better than the path-loss model, and the positioning accuracy increases with the number of the coarse site-surveying grids. Thus, the proposed semi-simulated method is potential to construct low-cost and high-resolution Wi-Fi fingerprint datasets.

The rest of the paper is structured as follows. After introducing the proposed SS-RSS in Section 2, Section 3 represents the performance analysis in detail. Section 4 draws the conclusion and future work. Some definitions and abbreviations are list in Table 1.

**Table 1.** List of abbreviations and definitions.

Definition	Explanation
APs	Wi-Fi Access Points
RSS	Received Signal Strength
SS-RSS	Semi-simulated <i>RSS</i> fingerprint construction method
Grids	A set of regular squares on an indoor map labeled sequences and position coordinates
Dense fingerprints	Fingerprints observed at dense grids
Coarse fingerprints	Fingerprints observed at coarse grids
Site-surveying grids	Grids with real-world <i>RSS</i> measurements
Non-site-surveying grids	Grids with simulated <i>RSS</i> values
Reference grids	Some nearby site-surveying grids used to simulate the dense fingerprints
Test-point	The point with the ground truth position and used to verify the positioning performance

## 2. The Proposed SS-RSS

This section introduces the proposed SS-RSS fingerprinting method. The procedure of the fingerprint construction is done into two phases: a coarse real-world fingerprint acquisition phase and a dense simulated fingerprint construction phase. A mobile device is used to acquire fingerprints at all coarse site-surveying grids (each grid with the known coordinates). The proposed semi-simulated method generates dense *RSS* fingerprints from the pre-processed real-world fingerprints. Then, indoor positioning is implemented by a general fingerprint matching algorithm (k-Nearest Neighbors). The pseudocode of SS-RSS is depicted in Figure 1 and Algorithm 1.

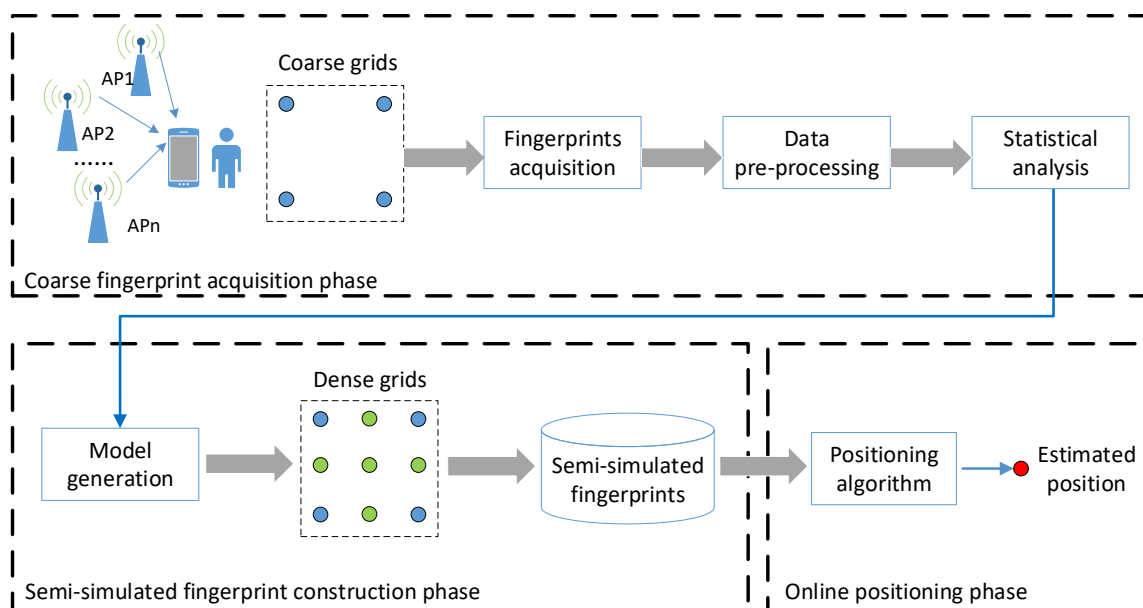


**Figure 1.** Architecture of the proposed Semi-simulated *RSS* Fingerprinting (SS-RSS) method, with the blue “o” denoting the site-surveying grids of real-world measurements, and the green “o” for the non-site-surveying grids with simulated Received Signal Strength (*RSS*) values.

As described in Figure 1, the SS-RSS can use either a path-loss model or quadratic polynomial fitting to estimate the *RSS* at the non-site-surveying grid according to some nearby site-surveying grids [25]. Moreover, from our real experiments, the results denote that the quadratic polynomial fitting method performs better than the path-loss model for the *RSS* simulation. Therefore, the SS-RSS method mentioned below is based on the quadratic polynomial fitting method if is not specifically stated.

**Algorithm 1** Pseudocode of SS-RSS Algorithm

---

**Input:** RSS values and coordinates of the site-surveying grids, coordinates of APs, coordinates of non-site-surveying grids

**Output:** Simulated RSS fingerprinting ( $F$ )

- 1: Initialize similarity set  $S$  as an empty set;
- 2: Initialize fingerprinting set  $F$  as an empty set;
- 3: **for** (each non-site-surveying grid  $P_i$  to be simulated) **do**
- 4: Initialize the RSS vector  $V$  simulated at grid  $P_i$ ;
- 5: **for** (each reachable AP  $R_j$  with known positions) **do**
- 6: **for** (each site-surveying grid  $T_k$  in the reference grids) **do**
- 7: Calculate the cosine similarity  $sim_{ijk}$  between  $P_i$  and  $T_k$  based on the coordinates of  $P_i$ ,  $T_k$  and  $R_j$ ;
- 8: Add  $sim_{ijk}$  into  $S$  (a higher value means higher similarity);
- 9: **end for**
- 10: Select  $\beta$  nearest points based on  $S$ ; (if  $\beta=2$  use the path-loss model, and if  $\beta=4$  use fitting method with quadratic polynomial);
- 11: Calculate the simulated RSS value  $R\hat{S}$  of  $P_i$  based on Equations (8) or (9);
- 12: Add the simulated RSS value  $R\hat{S}$  into  $V$ ;
- 13: **end for**
- 14: Add  $V$  into  $F$ ;
- 15: **end for**

---

## 2.1. Criterion for Reference Grids

In indoor scenarios, the RSS measurements are severely affected by the multipath effect (reflection, refraction, shadowing, scattering, etc.). The multipath effect generally results in a deviation between the theoretical signals and real-world RSS measurements, which is a nonlinear and heterogeneous model. To interpolate dense fingerprints, it needs to model the reference RSS values according to some site-surveying grids (namely, reference grids). The multipath effect is highly dependent on the surrounding environments; therefore, we propose to use cosine similarity to choose nearby grids to be the reference grids, with the cosine similarity expressed as

$$\text{sim}(X, Y) = \cos \theta = \frac{XY}{\|X\| \|Y\|}, \quad (1)$$

where  $X$  and  $Y$  refer the two vectors of the coordinates,  $\text{sim}(X, Y)$  represents the similarity of the two vectors, and a higher value means higher similarity.

Figure 2. depicts the schematic diagram of selecting the reference grids for the simulation of dense fingerprints. Suppose the RSS from the AP at one non-site-surveying grid in the corridor. Firstly, the cosine similarity (indicating the direction similarity) is used to sort the site-surveying grids. As displayed in Figure 2, the two nearest site-surveying grids are labeled as “1” and “2”, representing the nearest and the second nearest site-surveying grids to target simulation position.

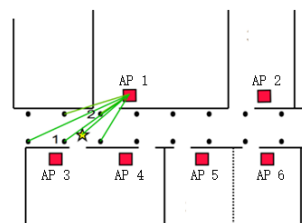


**Figure 2.** Schematic diagram for selecting the reference points based on the cosine similarity, with APs represented as the red “□”, the yellow “\*” as the non-site-surveying grids of the dense fingerprints (in other words, the grids needed to simulate RSS), the black dots as the site-surveying grids of the coarse fingerprints (the grid with real RSS measurements), and the green lines denote the transmission path between the AP and grid pair of the simulated or measured fingerprints.

### 2.2. Analytical Solution with A Path-Loss Model

According to the path-loss model [26], RSS can be estimated by

$$RSS(d) = RSS(d_0) - 10\eta \log_{10}\left(\frac{d}{d_0}\right) + \alpha, \tag{2}$$

where  $RSS(d_0)$  is the RSS measured at a reference distance  $d_0$  (usually 1 m),  $\eta$  is the path-loss exponent, and  $\alpha$  represents other losses including multipath and shadowing.

Then, the RSS can be simulated base on the path-loss model expressed by Equation (2),

$$\begin{cases} RSS_1 = RSS(d_0) - 10\eta \log_{10}\left(\frac{d_1}{d_0}\right) + \alpha, \\ RSS_2 = RSS(d_0) - 10\eta \log_{10}\left(\frac{d_2}{d_0}\right) + \alpha. \end{cases} \tag{3}$$

where  $RSS_1$  is the RSS measured at the distance  $d_1$ , and  $RSS_2$  is the RSS measured at the distance  $d_2$ . From Equation (3), one can derive the following function:

$$\frac{\log_{10}\left(\frac{d_1}{d_0}\right)}{\log_{10}\left(\frac{d_2}{d_0}\right)} = \frac{RSS(d_0) + \alpha - RSS_1}{RSS(d_0) + \alpha - RSS_2'} \tag{4}$$

Since  $d_0 = 1\text{ m}$ , one can get

$$\frac{\log_{10}(d_1)}{\log_{10}(d_2)} = \frac{\phi - RSS_1}{\phi - RSS_2'} \tag{5}$$

where  $\phi = RSS(d_0) + \alpha$ , it can be solved with respect to the RSS values and distances of the two most relevant site-surveying grids. Moreover, the final simulated RSS can be formulated as

$$\frac{\log_{10}(d^*)}{\log_{10}(d_1)} = \frac{\phi - RSS(d^*)}{\phi - RSS_1}, \tag{6}$$

where  $d^*$  is the distance between the non-site-surveying grid and the corresponding AP. Therefore, the RSS of the simulated fingerprint can be calculated by

$$RSS(d^*) = \phi - \frac{\log_{10}(d^*)(\phi - RSS_1)}{\log_{10}(d_1)}. \tag{7}$$

Equation (7) defines the RSS value at the simulated grid based on the  $\beta$  ( $\beta = 2$ ) most similar site-surveying grids with known RSS values and coordinates, given by

$$RSS(d^*) = \frac{RSS_2 \log_{10} \frac{d^*}{d_1} - RSS_1 \log_{10} \frac{d^*}{d_2}}{\log_{10} \frac{d_2}{d_1}}. \tag{8}$$

As a result, the simulated dense fingerprints can be constructed from measured coarse fingerprints.

### 2.3. Fitting Solution with a Quadratic Polynomial Function

Besides the aforementioned path-loss model, a fitting solution with a quadratic polynomial function can be used to estimate the RSS fingerprinting without strict geometry information. Similar to Algorithm 1 of the path-loss solution, the polynomial fitting consists of two phases.

Firstly, the  $\beta$  ( $\beta = 4$ ) reference grids are selected according to the proposed cosine similarity criterion. Then, the polynomial fitting method is applied to fit the relation curve between the RSS value and distance of the selected reference grids. In this work, the quadratic polynomial used in SS-RSS is expressed by

$$R\hat{S}S = c_2d^2 + c_1d + c_0, \{RSS_k\}_{k=1}^4, \quad (9)$$

where  $c_2$ ,  $c_1$ , and  $c_0$  are the coefficients of the polynomial depending on the selected 4 most similar reference grids  $\{RSS_k\}_{k=1}^4$ .

#### 2.4. Interpolation Solution with Matlab® 4 Griddata Method (V4)

The V4 method is a Greens' function based on the Biharmonic spline interpolation, which supporting 2-D interpolation. According to [27], Green functions of the Biharmonic operator, in one and two dimensions, are used for minimum curvature interpolation of irregularly spaced data points. The interpolating curve (or surface) is a linear combination of Green functions centered at each data point. In addition, in one (or two) dimensions this technique is equivalent to cubic spline (or bicubic spline) interpolation. However, it is more flexible than the spline method since both slopes and values can be used to find a surface. Moreover, noisy data can be fit in least squares sense by reducing the number of model parameters. These properties are well suited for interpolating irregularly spaced satellite altimeter profiles. Therefore, in the RSS fingerprint construction phase, the V4 interpolation method can be used to generate dense fingerprints.

#### 2.5. Positioning Algorithm

For the simplicity of the positioning algorithm, we used k-nearest neighbor (KNN) [28] to validate the proposed RSS fingerprint generating method, which is described as follows:

- (a) Select  $K$  nearest neighbors of the RSS vector from the RSS fingerprint dataset;
- (b) After  $K$  nearest neighbors are selected as the  $K$  possible target positions, the final position is estimated by the average of the  $K$  positions as

$$D_{k+1} = \frac{1}{K} \sum_{j=1}^K D_j, \quad (10)$$

where  $D_j$  is the position of the  $j$ th nearest neighbor, and  $D_{k+1}$  is the final position of the mobile target at time sequence  $k + 1$ .

### 3. Performance Analysis

In this section, a mobile indoor experiment is carried out to compare the results among the dense fingerprinting method, the coarse fingerprinting method, the purely simulated fingerprinting method, and the proposed semi-simulated construction from the coarse fingerprinting.

#### 3.1. RSS-Distance Ranging Model

The measurements of 16 test distance from the range of 0.5 m to 8 m are used to fitting the RSS-distance model, which measures for 1 min at each test distance. Figure 3 illustrates the curve fitting results between the average RSS value and the corresponding distance. The two fitting models (the path loss model and the quadratic polynomial model) are chosen to minimize the root mean squared error (RMSE), which is denoted by  $RMSE = \sqrt{E[(R\hat{S}S - RSS^*)^2]}$  with the theoretical  $RSS^*$  and the estimated  $R\hat{S}S$  [29]. The benchmark path-loss curve is formulated as

$$RSS = -47.73 - 18.5828 \log_{10}d + 2.3569. \quad (11)$$

Similarly, the blue solid line in Figure 3 represents the fitting curve of the polynomial of

$$RSS = 0.3324d^2 - 5.5051d + 39.9167. \quad (12)$$

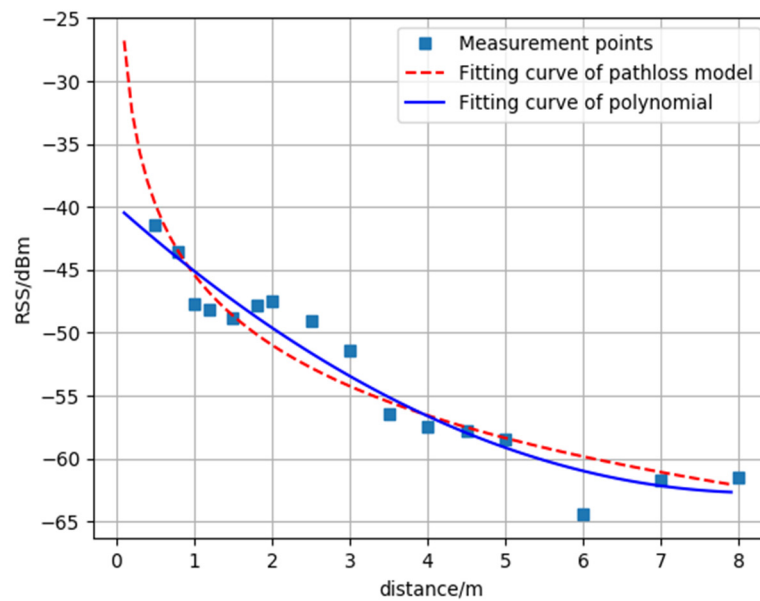


**Figure 3.** Relationship between RSS and the distance of the experiment data. The solid “□” represents the average RSS at each test distance, the red dotted line shows the path-loss curve, and the blue solid line represents the fitting curve of the quadratic polynomial.

### 3.2. Experiments Implementation

The experiment is carried out in a typical laboratory room in our institute building. As described in Figure 4, the experiment room is about 10 m × 15 m with five APs on the tables.

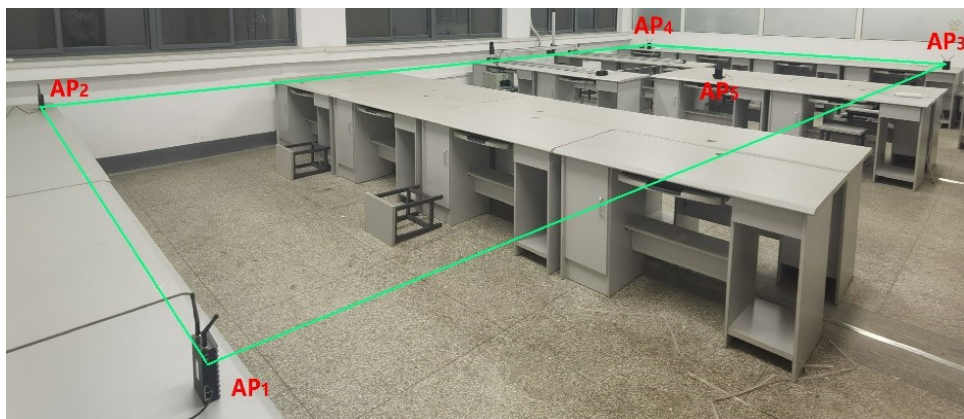
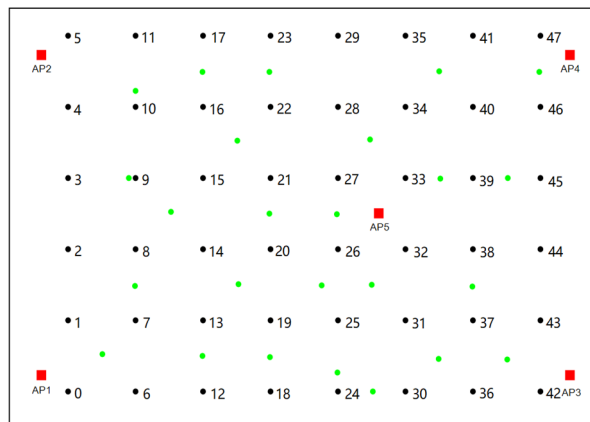


**Figure 4.** Diagram of the indoor test environment and APs deployment.

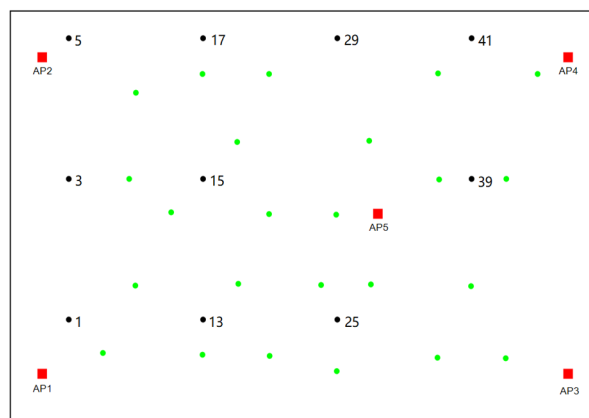
We compared four fingerprinting database conduction methods, which are the measured dense fingerprints, the measured coarse fingerprints, the spatial interpolation fingerprints with the measured coarse fingerprints, and the proposed semi-simulated fingerprints, respectively.

- (1) The measured dense fingerprints of our experiment are shown in Figure 5, with the site-surveying grids (the labeled black dots) and APs (the red blocks). The size of each grid is about 1.2 m × 1.1 m, and the fingerprint acquisition at each grid maintains more than 10 s.
- (2) The measured coarse fingerprints are demonstrated in Figure 6, with the site-surveying grids (the labeled black dots) and APs (the red blocks). The size of the coarse grid is two times larger than the dense grid.
- (3) Given the measured coarse fingerprints, the spatial interpolation fingerprints or the proposed SS-RSS fingerprints are shown in Figure 7, with the site-surveying grids (the labeled black dots)

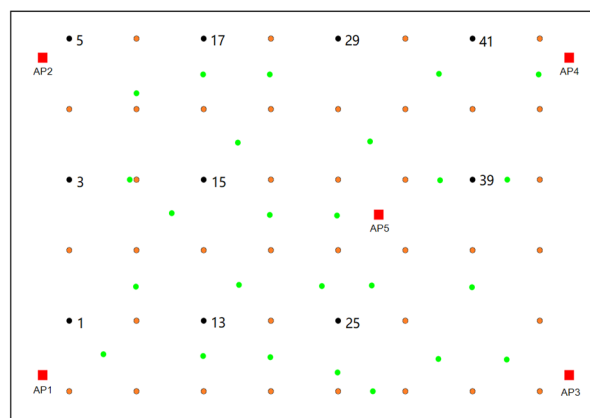
and APs (the red blocks), and the simulated fingerprinting grids (the pink dots). The size of the simulated fingerprint grid is the same as the dense site-surveying grid.



**Figure 5.** Distribution of the dense acquisition for Wi-Fi fingerprints, with the red “□” representing the five APs, the black dots with the labeled number for the dense site-surveying grids, the green dots for the test-points.



**Figure 6.** Distribution of the coarse acquisition for Wi-Fi fingerprints, with the red “□” representing the five APs; the black dots with the labeled number for the coarse site-surveying grids; the green dots for the test-points.



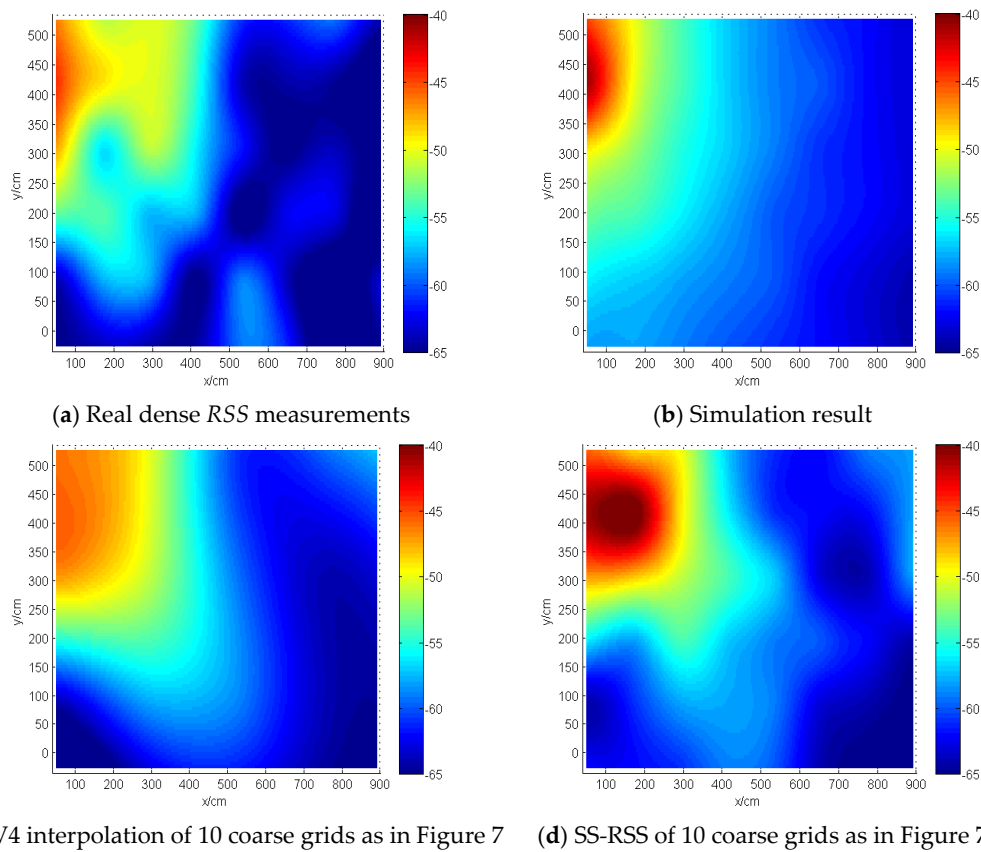
**Figure 7.** Distribution of the spatial interpolation fingerprints and the SS-RSS fingerprints. The red “□” represents the five APs; the black dots with labeled numbers denote the coarse grids; the pink dots represent the simulated fingerprints of the spatial interpolation or the SS-RSS construction; the green points represent the test-points.

Figure 8 displays the RSS distribution of one Wi-Fi AP using different fingerprint construction methods. Figure 9 and Table 2 illustrate the RSS difference (*diff*) between the fingerprint construction methods and the measured RSS.

$$diff = R\hat{S}S - RSS^*, \tag{13}$$

where  $R\hat{S}S$  represents the estimated RSS from based on the fingerprint construction and  $RSS^*$  represents the real RSS obtained from the real fingerprint measurements.

From Figures 8 and 9, one can derive that the RSS distribution constructed by the SS-RSS is more similar to the real dense RSS distribution, and the coarse fingerprint grids with interpolation get smaller differences to the real RSS values.



**Figure 8.** Two dimensions (2D) heat map of the Wi-Fi RSS distribution from one AP of four fingerprinting database conduction methods.

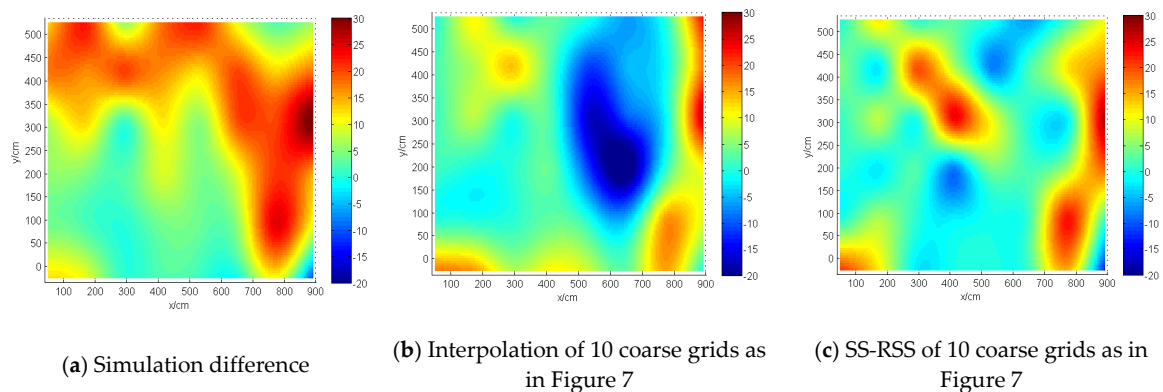


**Figure 9.** 2D heat map of the average RSS difference (*diff*) from 5 Aps.

**Table 2.** Typical values of the RSS fingerprint construction methods.

Fingerprinting Construction Method	MAE (dBm)	RMSE (dBm)	Max (dBm)
SS-RSS	5.97	6.88	27.71
Simulation	10.87	7.12	30.76
Coarse measured fingerprints	6.55	8.31	26.86

### 3.3. Experiment with Nearest Neighbor Rule

Table 3 lists the positioning results of different fingerprint construction methods using KNN, representing that the quadratic polynomial fitting method performs better than the path-loss model in the SS-RSS construction. Set a small value of  $k$  means that noise will have a higher influence on the positioning result, whereas a large value makes it computationally expensive. For our results, with the increasing number of  $k$ , the positioning accuracy improves a little. We suppose to determine  $k < 10$  as the parameter of this experiment scenario.

**Table 3.** Positioning results of different fingerprint construction methods based on  $k$ -nearest neighbor (KNN) versus the number of nearest neighbors.

Nearest-Neighbor Rule $k$	Fingerprinting Construction Method	MAE (m)	RMSE (m)	90%-Tile (m)
Case 1 $k = 2$	Dense site-surveying grids	1.20	0.74	1.88
	Coarse site-surveying grids	1.45	0.73	2.44
	SS-RSS (Equation (8))	1.51	0.97	2.91
	SS-RSS (Equation (9))	1.26	0.50	1.76
	SS-RSS (V4)	1.19	0.63	1.88
	Simulation (Equation (11))	1.45	0.89	2.64
	Simulation (Equation (12))	1.26	0.76	2.28
Case 2 $k = 3$	Dense site-surveying grids	1.04	0.61	1.51
	Coarse site-surveying grids	1.35	0.81	2.21
	SS-RSS (Equation (8))	1.33	0.90	2.58
	SS-RSS (Equation (9))	1.19	0.60	2.06
	SS-RSS (V4)	1.14	0.56	1.61
	Simulation (Equation (11))	1.34	0.90	2.58
	Simulation (Equation (12))	1.23	0.85	2.17
Case 3 $k = 4$	Dense site-surveying grids	1.03	0.59	1.80
	Coarse site-surveying grids	1.70	0.97	2.91
	SS-RSS (Equation (8))	1.37	0.83	2.63
	SS-RSS (Equation (9))	1.11	0.59	1.86
	SS-RSS (V4)	1.18	0.65	1.82
	Simulation (Equation (11))	1.22	0.89	2.51
	Simulation (Equation (12))	1.20	0.78	2.29
Case 4 $k = 5$	Dense site-surveying grids	0.98	0.56	1.54
	Coarse site-surveying grids	1.90	1.03	3.03
	SS-RSS (Equation (8))	1.36	0.75	2.29
	SS-RSS (Equation (9))	1.06	0.52	1.56
	SS-RSS (V4)	1.11	0.66	1.85
	Simulation (Equation (11))	1.27	0.86	2.46
	Simulation (Equation (12))	1.25	0.75	2.20

With different nearest-neighbor rules, one can note that the SS-RSS (V4) method outperforms the coarse fingerprints and purely simulated fingerprints and is comparable to the real dense fingerprints. It reveals that the SS-RSS (V4) methods make use of both the direction and distance weighting. The SS-RSS methods of either Equations (8) or (9) explore the direction similarity, which can approximate the uneven indoor RSS distribution.

### 3.4. Different Number of the Coarse Fingerprint Grids for SS-RSS

We chose different numbers of the coarse fingerprint grids from the dense site-surveying grids to test the proposed semi-simulated method. In addition, we compare the proposed semi-simulated

method among different fingerprint construction methods based on 10 selected coarse grids (e.g., 1, 3, 5, 13, 15, 17, 25, 29, 39, and 41). Meanwhile, we verify the performance of the proposed method based on different selected coarse site-surveying grids (see Figure 10).

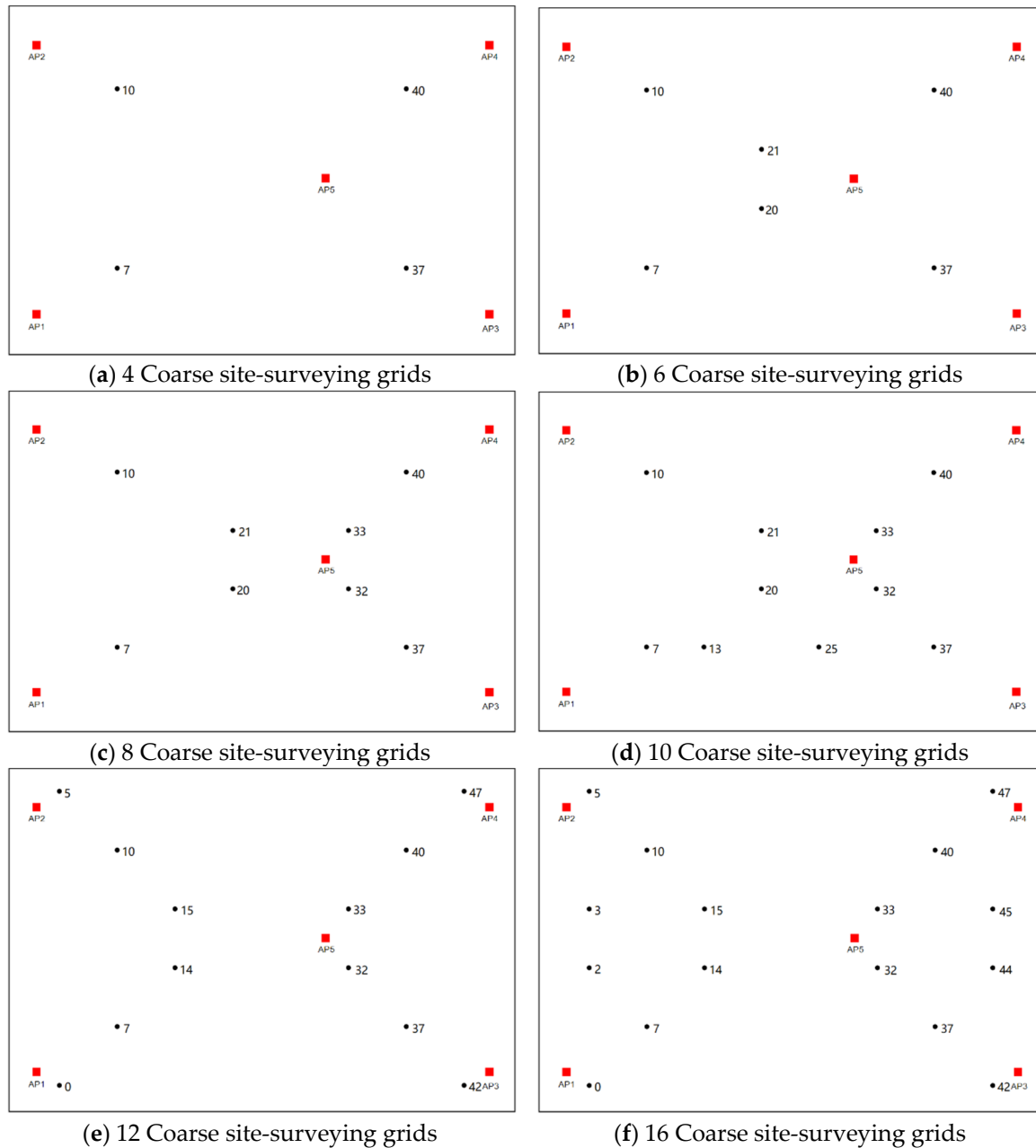


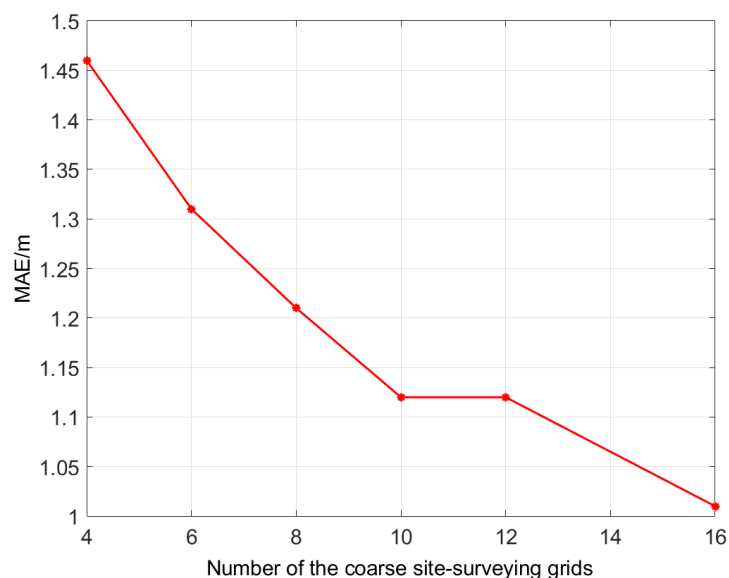
Figure 10. SS-RSS based on the fingerprints of increasing numbers of coarse site-surveying grids.

For the comparison of the different numbers of the chosen coarse site-surveying grids to generate the site-surveying fingerprint dataset, we define  $k$  of the KNN equals to four. The results of mean absolute error (MAE), root mean square error (RMSE), and 90%-percentile on the SS-RSS are shown in Table 4, e.g.,  $N_c = 4$  represents that the number of the coarse site-surveying grids is 4. The average positioning accuracy achieves up to 1.01 m with the semi-simulation ratio of 66.6% (defined as the ratio of the simulated RSS fingerprints to all fingerprints, e.g., the 16 coarse site-surveying grids to 48 grids is 66.6%).

**Table 4.** KNN positioning accuracy of different fingerprint construction methods.

KNN Positioning with Different Fingerprint Construction Methods	MAE (m)	RMSE (m)	90%-Tile (m)
Dense site-surveying grids (48 grids)	1.03	0.59	1.80
Coarse site-surveying grids (Nc = 4)	2.64	1.06	3.67
SS-RSS (Nc = 4)	1.46	0.93	2.64
Coarse site-surveying grids (Nc = 6)	2.00	1.05	2.75
SS-RSS (Nc = 6)	1.31	0.85	2.12
Coarse site-surveying grids (Nc = 8)	1.91	0.91	3.00
SS-RSS (Nc = 8)	1.21	0.94	2.44
Coarse site-surveying grids (Nc = 10)	1.63	0.82	2.55
SS-RSS (Nc = 10)	1.12	0.44	1.60
Coarse site-surveying grids (Nc = 12)	1.59	0.91	2.54
SS-RSS (Nc = 12)	1.12	0.58	1.76
Coarse site-surveying grids (Nc = 16)	1.66	0.85	2.67
SS-RSS (Nc = 16)	1.01	0.67	1.71

Figure 11 depicts the relation curve between MAE and  $N_c$ . It is clear that the positioning accuracy decrease with the  $N_c$ . The results indicate, overall, that the KNN positioning using the SS-RSS fingerprint construction achieve comparable accuracy as the dense site-surveying fingerprinting method and performs better than the coarse site-surveying fingerprinting method.

**Figure 11.** Mean absolute error (MAE) of SS-RSS Versus the number of the coarse site-surveying grids.

To verify the proposed construction method, we compare the cumulative distribution function (CDF) of the positioning errors from different fingerprint construction methods, as displayed in Figure 12. For example, as for the proposed semi-simulated method, if the positioning error is within 1.5 m, the probability of it is about 0.96. As revealed by Figure 12, the curve of SS-RSS based on the polynomial method is close to the dense site-surveying method, which indicates that the proposed SS-RSS performs effectively in the fingerprint database construction.

The above comparison can be summarized as follows:

- (1) The quadratic polynomial fitting method performs better than the path-loss model in both the semi-simulated construction model and the simulation construction model in this paper.

- (2) The proposed SS-RSS can improve positioning accuracy compare with either a coarse construction method or pure simulations, indicating that the cosine similarity methods make the simulated fingerprints more reality.
- (3) The mean absolute error of positioning decreases with the increase of the number of the coarse site-surveying grids for SS-RSS from the experiment results.
- (4) By comparing the aforementioned methods of Wi-Fi fingerprint construction, the proposed method combines the real Wi-Fi fingerprinting acquisitions and the semi-simulation. As a result, the accuracy of the proposed method is improved, and the workload of Wi-Fi fingerprint construction is reduced.

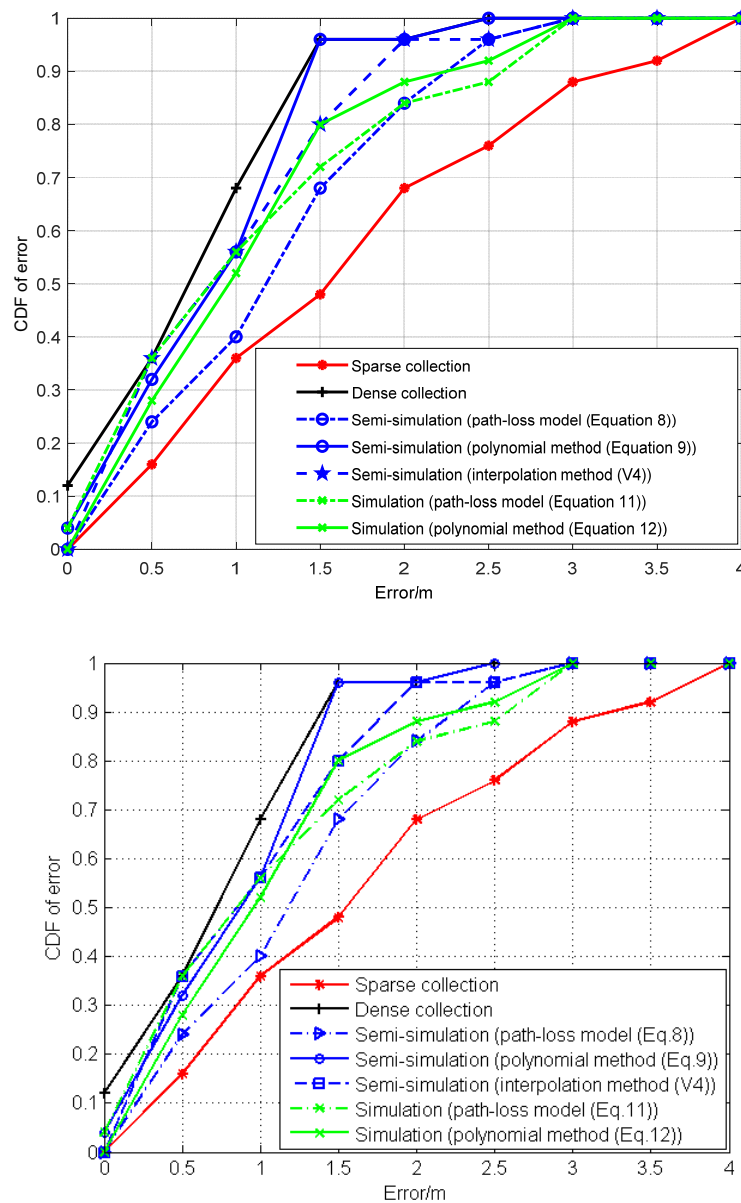


**Figure 12.** Cumulative distribution function of the positioning errors from different RSS fingerprint dataset construction methods (with 10 coarse site-surveying grids).

Overall, the reasons why the proposed SS-RSS performs better are: the cosine similarity can ensure direction consistency to make the transmission path consistency. Then, the coarse site-surveying grids, which are applied to generate fingerprinting by SS-RSS, can reduce the estimation error caused by real positioning environments. Moreover, the quadratic polynomial fitting method used in the proposed

SS-RSS is likely to fit the relation between RSS and distance better than the path-loss model. Therefore, the coarse Wi-Fi fingerprints can provide a practical standard for SS-RSS method, which can combine the real-world signal propagation with the theoretical propagation model to improve the accuracy of the constructed Wi-Fi fingerprinting of indoor multipath scenarios.

#### 4. Conclusions and Future Work

This study proposes the semi-simulation to construct dense fingerprints from coarse fingerprinting grids, aiming at fine resolutions and low efforts for Wi-Fi positioning. It compares the RSS fingerprint constructions based on the standard log-distance path-loss model, the spatial interpolation methods, and the semi-simulation from the real coarse fingerprint. The experiment results reveal that the cosine similarity fitting can make use of the direction consistency to real fingerprints. Moreover, the quadratic polynomial fitting of the proposed semi-simulated fingerprint construction can fit the RSS uncertainty of the given indoor scenarios. Overall, the semi-simulated fingerprinting provides a low cost and practical strategy for a fast establishment and update of fingerprinting-based positioning, which combines the real-world signal propagation with the theoretical model. The average positioning accuracy achieves up to 1.01 m with 66.6% of the semi-simulation ratio. However, it takes much work force and time to maintain the Wi-Fi fingerprinting dataset in this research. Therefore, further work will explore a self-adapting radio map of a given indoor multipath environment to conquer variants of fingerprints in large areas.

**Author Contributions:** Conceptualization, Y.Y.; methodology, P.D.; software, P.D.; validation, Y.Y. and P.D.; formal analysis, H.H.; investigation, M.W.; data curation, Y.Y, P.D. and Y.K.; writing—original draft preparation, X.X.; writing—review and editing, Y.Y. and P.D.; supervision, H.H.; project administration, M.W.; funding acquisition, H.H. All authors have read and agreed to the published version of the manuscript.

**Funding:** This work was funded by the projects of the National Key Research and Development Plan of China (Grant Number: 2016YFB0502103), the National Natural Science Foundation of China (Grant Number: 61701237), the National Natural Science Foundation of China (61703098).

**Conflicts of Interest:** The authors declare no conflict of interest.

#### References

1. Ashraf, I.; Hur, S.; Park, Y. Smartphone Sensor Based Indoor Positioning: Current Status, Opportunities, and Future Challenges. *Electronics* **2020**, *9*, 891. [[CrossRef](#)]
2. Lin, K.; Chen, M.; Deng, J.; Hassan, M.M.; Fortino, G. Enhanced Fingerprinting and Trajectory Prediction for IoT Localization in Smart Buildings. *IEEE Trans. Autom. Sci. Eng.* **2016**, *13*, 1294–1307. [[CrossRef](#)]
3. Yang, C.; Shao, H.-R. WiFi-based indoor positioning. *IEEE Commun. Mag.* **2015**, *53*, 150–157. [[CrossRef](#)]
4. Montoliu, R.; Sansano-Sansano, E.; Gascó, A.; Belmonte, O.; Caballer, A. Indoor Positioning for Monitoring Older Adults at Home: Wi-Fi and BLE Technologies in Real Scenarios. *Electronics* **2020**, *9*, 728. [[CrossRef](#)]
5. Khalifa, S.; Hassan, M.; Hassan, M. Evaluating mismatch probability of activity-based map matching in indoor positioning. In Proceedings of the International Conference on Indoor Positioning and Indoor Navigation (IPIN), Sydney, Australia, 13–15 November 2012.
6. Xue, M.; Sun, W.; Yu, H.; Tang, H.; Lin, A.; Zhang, X.; Zimmermann, R. Locate the Mobile Device by Enhancing the WiFi-Based Indoor Localization Model. *IEEE Int. Things J.* **2019**, *6*, 8792–8803. [[CrossRef](#)]
7. Wu, C.; Yang, Z.; Liu, Y. Smartphones Based Crowdsourcing for Indoor Localization. *IEEE Trans. Mob. Comput.* **2015**, *14*, 444–457. [[CrossRef](#)]
8. Zafari, F.; Gkelias, A.; Leung, K.K. A Survey of Indoor Localization Systems and Technologies. *IEEE Commun. Surv. Tutorials* **2019**, *21*, 2568–2599. [[CrossRef](#)]
9. Talvitie, J.; Renfors, M.; Lohan, E.S. Distance-Based Interpolation and Extrapolation Methods for RSS-Based Localization with Indoor Wireless Signals. *IEEE Trans. Veh. Technol.* **2015**, *64*, 1340–1353. [[CrossRef](#)]
10. Zhou, S.; Wang, B.; Mo, Y.; Deng, X.; Yang, L.T. Indoor Location Search Based on Subarea Fingerprinting and Curve Fitting. In Proceedings of the IEEE 10th International Conference on High Performance Computing and Communications & IEEE International Conference on Embedded and Ubiquitous Computing, Zhangjiajie, China, 13–15 November 2013.

11. Li, L.; Guo, X.; Ansari, N.; Li, H. A Hybrid Fingerprint Quality Evaluation Model for WiFi Localization. *IEEE Int. Things J.* **2019**, *6*, 9829–9840. [[CrossRef](#)]
12. Jun, J.; He, L.; Gu, Y.; Jiang, W.; Kushwaha, G.; Vipin, A.; Cheng, L.; Liu, C.; Zhu, T. Low-Overhead WiFi Fingerprinting. *IEEE Trans. Mob. Comput.* **2018**, *17*, 590–603. [[CrossRef](#)]
13. Cidronali, A.; Collodi, G.; Lucarelli, M.; Maddio, S.; Passafiume, M.; Pelosi, G. Assessment of Anchors Constellation Features in RSSI-Based Indoor Positioning Systems for Smart Environments. *Electronics* **2020**, *9*, 1026. [[CrossRef](#)]
14. Liu, W.; Liu, H.; Wen, L.; Wang, L. A Scalable Lightweight Radio Fingerprint Map Construction Method. *Dianzi Yu Xinxi Xuebao J. Electron. Inf. Technol.* **2018**, *40*, 306–313.
15. Belmonte-Fernández, Ó.; Montoliu, R.; Torres-Sospedra, J.; Sansano-Sansano, E.; Chia-Aguilar, D. A radiosity-based method to avoid calibration for indoor positioning systems. *Expert Syst. Appl.* **2018**, *105*, 89–101. [[CrossRef](#)]
16. Lim, J.-S.; Yoon, G.-W.; Han, D.-S.; Jang, W.-H. Radio Map Update Automation for WiFi Positioning Systems. *IEEE Commun. Lett.* **2013**, *17*, 693–696. [[CrossRef](#)]
17. Jung, S.H.; Han, D. Automated Construction and Maintenance of Wi-Fi Radio Maps for Crowdsourcing-Based Indoor Positioning Systems. *IEEE Access* **2018**, *6*, 1764–1777. [[CrossRef](#)]
18. Ismail, A.; Kitagawa, H.; Tasaki, R.; Terashima, K. WiFi RSS fingerprint database construction for mobile robot indoor positioning system. In Proceedings of the IEEE International Conference on Systems, Man, and Cybernetics (SMC), Budapest, Hungary, 9–12 October 2016.
19. Zhang, P.; Zhao, Q.; Li, Y.; Niu, X.; Zhuang, Y.; Liu, J. Collaborative WiFi Fingerprinting Using Sensor-Based Navigation on Smartphones. *Sensors* **2015**, *15*, 17534–17557. [[CrossRef](#)]
20. Chen, L.; Li, B.; Zhao, K.; Rizos, C.; Zheng, Z. An Improved Algorithm to Generate a Wi-Fi Fingerprint Database for Indoor Positioning. *Sensors* **2013**, *13*, 11085–11096. [[CrossRef](#)]
21. Liu, Y.; Sharan Sinha, R.; Liu, S.-Z.; Hwang, S.-H. Side-Information-Aided Preprocessing Scheme for Deep-Learning Classifier in Fingerprint-Based Indoor Positioning. *Electronics* **2020**, *9*, 982. [[CrossRef](#)]
22. Abed, A.; Abdel-Qader, I. RSS-Fingerprint Dimensionality Reduction for Multiple Service Set Identifier-Based Indoor Positioning Systems. *Appl. Sci.* **2019**, *9*, 3137. [[CrossRef](#)]
23. Wang, B.; Zhou, S.; Yang, L.T.; Mo, Y. Indoor positioning via subarea fingerprinting and surface fitting with received signal strength. *Pervasive Mob. Comput.* **2015**, *23*, 43–58. [[CrossRef](#)]
24. Marco, N.M.; Hiram, H.R.; Cesar, T.H.; Heidy, M.C.; Yuriria, C.P. On-Device Learning of Indoor Location for WiFi Fingerprint Approach. *Sensors* **2018**, *18*, 2202.
25. Hoang, M.T.; Zhu, Y.; Yuen, B.; Reese, T.; Dong, X.; Lu, T.; Westendorp, R.; Xie, M. A Soft Range Limited K-Nearest Neighbours Algorithm for Indoor Localization Enhancement. *IEEE Sens. J.* **2019**, *18*, 10208–10216. [[CrossRef](#)]
26. Wang, Y.; Jia, X.; Lee, H.K. An indoor wireless positioning system based on wireless local area network infrastructure. *Univ. Technol. Dresden Ger. Univ. Technol.* **2003**, *1*, 5–18.
27. Sandwell, D. Biharmonic spline interpolation of GEOS-3 and SEASAT altimeter data. *Geophys. Res. Lett.* **1987**, *14*, 139–142. [[CrossRef](#)]
28. Wang, B.; Gan, X.; Liu, X.; Yu, B.; Jia, R.; Huang, L.; Jia, H. A Novel Weighted KNN Algorithm Based on RSS Similarity and Position Distance for Wi-Fi Fingerprint Positioning. *IEEE Access* **2020**, *8*, 30591–30602. [[CrossRef](#)]
29. Feng, C.; Au, W.S.A.; Valaee, S.; Tan, Z. Received-Signal-Strength-Based Indoor Positioning Using Compressive Sensing. *IEEE Trans. Mob. Comput.* **2012**, *11*, 1983–1993. [[CrossRef](#)]

